Acknowledgements

I would like to first thank Dr. Stephen Hursting for all of his support, patience, and guidance over the course of the last three years and especially with the unpredictable turns my project took. This lab provides the unique opportunity for undergraduates to conduct rigorous, professional level research and develop a true passion for all the nuances of research science, and without Dr. Hursting I would have never had this experience. I am further grateful for the direction and advice given by my graduate mentor and close friend, Shan McDonell. Every lab technique and almost all of my lab knowledge has come from his enthusiasm for science and academic research, and I am appreciative of all the care and effort he puts into research as well as the success of the entire lab. From all of our time together inside and outside of lab, I know our bond will continue to grow and there will be plenty more Bandido's Fridays to come. Additionally, I would like to recognize Dr. Michael Coleman and Dr. Alyssa Cozzo for always challenging me, motivating me, providing feedback, and allowing me to endlessly interrupt them with questions to help me with this project. Lastly, I want to thank my friends and family for their constant love and encouragement throughout my undergraduate career.

Abstract

Background: Obesity is associated with increased risk and poor prognosis of triple negative breast cancer (TNBC), a highly aggressive subtype of breast cancer with high rates of metastasis and recurrence. Previous research from our lab showed calorie restriction (CR) has an antitumorigenic effect against TNBC, although mechanisms remain unclear. We hypothesize that CR may facilitate this anticancer effect, at least in part, via upregulation of microRNA (miR)-15b and subsequent disruption of IGF-1 system activation.

Methods: cBioPortal, TargetScan, miRTarBase, and various TCGA data sets were utilized to conduct *in silico* analysis of potential genes and target pathways associated with miR-15b expression, especially along the PI3K/Akt/mTOR pathway. To mimic caloric restriction *in vitro*, M6 and M6C cells derived from the C3-Tag series progression cell were treated with several nutrient restricted medias including reduced serum, BMS754807 (inhibitor of IGF1-R), IGF-1, and different combinations of these three conditions. To characterize the impact of caloric restriction on these cells and their potential mechanistic action, qPCR was performed on miRNA and mRNA collected to determine fluctuations in levels of miR-15b and IGF1-R.

Results: The qPCR analysis performed *in vitro* did not yield any statistically significant results demonstrating the impact of caloric restriction on miR-15b or IGF1-R. However, *in silico* analyses revealed that miR-15b overexpression in human breast tumors was associated with increased expression of genes associated with regulation of breast cancer cell proliferation, while decreased miR-15b was associated with enhanced growth factor signaling and epithelial-to-mesenchymal transition.

Conclusion: *In silico* studies suggest the anticancer effects of CR in a murine model of TNBC may be mediated, at least in part, through increased miR-15b expression and subsequent targeting of the IGF1 axis regulating downstream genes involved in breast cancer cell proliferation and progression. However, several sources of error could have impacted the *in vitro* component of this study, indicating that further analyses are necessary to confirm the interaction amongst caloric restriction, miR-15b, and IGF-1 system activation of the PI3K/Akt/mTOR pathway.

Introduction

Triple-negative breast cancer lacks adequate molecular targets. The most diagnosed cancer in women and the second-most deadly only behind lung cancer, breast cancer is a highly devastating disease that impacts every 1 in 8 women born in the United States (1,2). Comprising approximately 20% of diagnosed breast cancers, triple negative breast cancer (TNBC) is a highly aggressive breast cancer subtype with a greater potential to metastasize and recur than all other subtypes. While the five-year survival rate for other subtypes averages at 93%, the five-year survival rate for TNBC is only 77% (3). Additionally, black women are twice as likely to be diagnosed with TNBC than white women (4). The prognosis for TNBC is particularly devastating because it lacks the three molecular targets that can be inhibited by hormone-targeted therapies (estrogen, progesterone, and HER2/neu receptors), leaving patients no other option than undergoing the traditional yet physically harmful process of cytotoxic chemotherapy (5). Because of the numerous negative side-effects associated with chemotherapy treatment such as anemia, severe fatigue, and alopecia, and the known disparities in disease burden across racial and ethnic groups, researchers have long sought more effective, alternative treatments with fewer adverse effects.

Dietary energy balance impacts cancer risk and progression. Obesity is an established risk factor for breast cancer development (5-7), and weight gain throughout life, as well as after diagnosis, has been shown to decrease survival in both pre- and post-menopausal breast cancer patients (8-10). Furthermore, obesity has been shown to modulate the severity of symptoms present in patients with breast cancer (6) and post-menopausal patients diagnosed with TNBC specifically are more likely to be overweight/obese than at a healthy weight (7). For each BMI unit increase, the breast cancer mortality risk increases by 8-29%, dependent on the initial BMI taken

for a patient (8). Additionally, obesity has been shown to drive indicators of poorer prognoses such as tumor size, tumor grade, and metastasis (9). It is also known to play a role in increasing several pro-inflammatory pathways that can contribute to heterogeneity within the tumor microenvironment by maintaining cancer stem cell populations, leading to tumor development and invasion (10).

One therapeutic avenue that has shown promise in treatment of TNBC while reducing the consequences of cytotoxic chemotherapy is dietary caloric restriction (CR). In CR, a patient receives complete nutrition while reducing calorie intake (11). Previous studies in the Hursting lab have indicated that CR diets in mouse models of TNBC not only significantly improve the length of tumor-free survival and overall survival of mice, but also decrease total tumor count and average secondary tumor weight (12). This data is shown in figure 1.

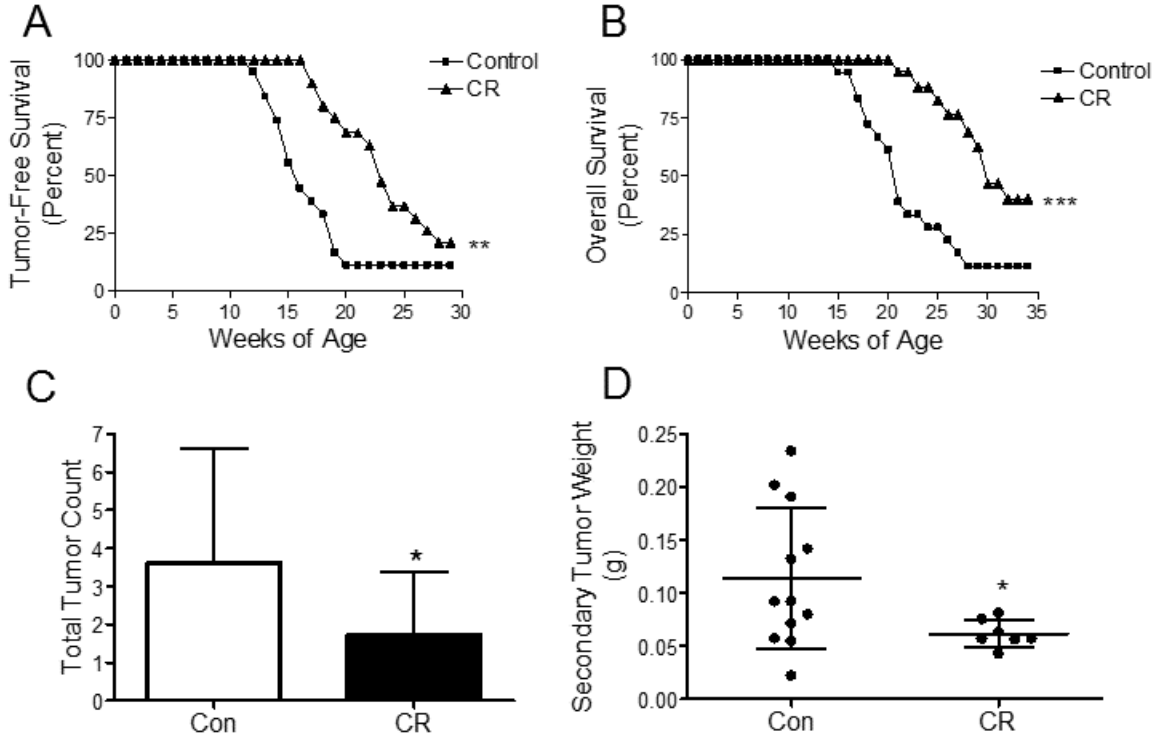

Figure 1: Survival curve depicting improved tumor-free survival (A) and overall survival (B) from *in vivo* studies done on C3(1)-Tag spontaneous tumor mouse models fed a 30% CR diet compared to a control *ad libitum* diet. Mice on CR diets also had lower overall tumor count (C) and decreased secondary tumor weight (D). *, P<0.05; **, P<0.001; ***, P<0.0001.

IGF signaling is vital to cancer development. Synthesized in the liver, IGF-1 is a peptide hormone integral to mediating somatic development initially stimulated by growth hormone, and is especially important in regulating the cell cycle process. CR in both humans and animal models decreases circulating levels of IGF-1 (Figure 2). IGF-1 functions by binding to insulin-like growth factor 1 receptor (IGF-1R) to activate the phosphatidylinositol-3 kinase (PI3K)/Akt pathway, which controls multiple downstream mediators such as the mammalian target of rapamycin (mTOR). This tyrosine kinase receptor cascade pathway is vital to maintaining appropriate nutrient levels to control development, protein synthesis, and overall survival in the cell (14). IGF signaling is important in tumor development because it increases cell proliferation while inhibiting apoptosis in cancer cells. Additionally, IGF signaling is frequently high in patients whose lifestyles are characterized by minimal exercise and dietary choices high in fat and animal proteins (15).

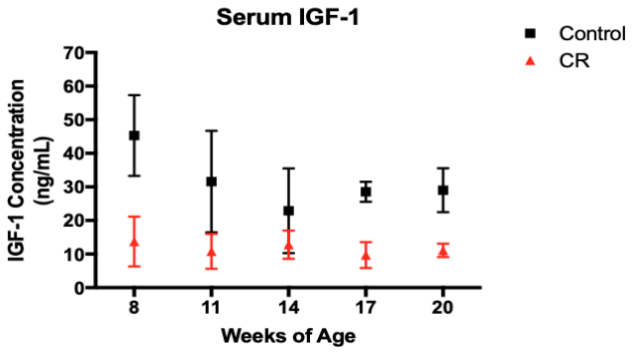

Figure 2: Plot displaying increased concentration of IGF-1 present in the circulation of mice fed a control diet (black) vs a CR diet (red).

In breast cancer, several studies have shown that IGF-1 levels play a crucial role in mammary tumorigenesis. Studies performed in murine models have demonstrated that mammary tumor development was impeded in mice with reduced IGF-1 levels (16). Moreover, the ability to undergo oncogenic transformation depends on the IGF-1/IGF-1R interaction and activation of downstream signaling (17). In addition, another study specifically examined IGF-1's role in seven different triple negative breast cancer cell lines. The results of this study displayed that IGF-1 increased the proliferation and survival rate of all cell lines compared to their controls (18). Furthermore, it is widely recognized that elevated levels of both systemic and tumor IGF-1 are

strong determinants of a patient's prognosis following diagnosis with triple negative breast cancer (19).

IGF-1R is a potential target of microRNA-15b. While there are several molecular targets under CR's comprehensive reach, previous studies performed in our laboratory have led us to suspect that miRNA-15b may be a key mediator of CR's antitumorigenic effects in TNBC. miRNAs are small strands (~22 nucleotides long) of highly conserved non-coding RNA that are important in gene regulation. They are generated from a set of precursors that undergo several cleavage events before arriving at the final miRNA form (20). miRNAs target mRNA transcripts by binding to the 3' UTR of the mRNA with their seed sequences, which are usually nucleotides 2-7 of the miRNA (21). In most animal models, the seed sequences are partially complementary (meaning the entire seed sequence is not a perfect match), which leads to partial mRNA degradation or translational repression, leading to reduced protein expression rather than complete elimination of expression (22). However, in the case of full complementarity there can be total destruction of the mRNA sequence. Regardless of the extent of a miRNA's complementarity, any deterioration that occurs is completed as complementary sequences lead to formation of the RISC complex (RNA-induced silencing complex), which consists of a group of ribonucleoproteins that position a gene target for recognition and cleavage by other Argonaute proteins (23). Previous work completed in the Hursting Lab has shown that in the C3(1)-Tag mouse models fed either a control diet of a 30% CR diet, gene expression of miR-15b was significantly increased while expression of IGF1-R was significantly reduced in relative protein quantity and gene expression. This relationship is depicted in figure 3. miR-15b's inhibitory effect towards this transmembrane receptor may be the mechanism by which CR's anti-cancer and tumor suppressing processes are occurring. With decreased receptor expression, IGF-1 is unable to exert its effects via the PI3K/Akt/mTOR

pathway to enhance proliferation, growth, survival, and development of TNBC cells. TNBC's deadly progression has a clear correlation with obesity, and it is paramount that the mechanism by which CR and mIR-15b operate is understood in order to instill a more effective treatment regimen.

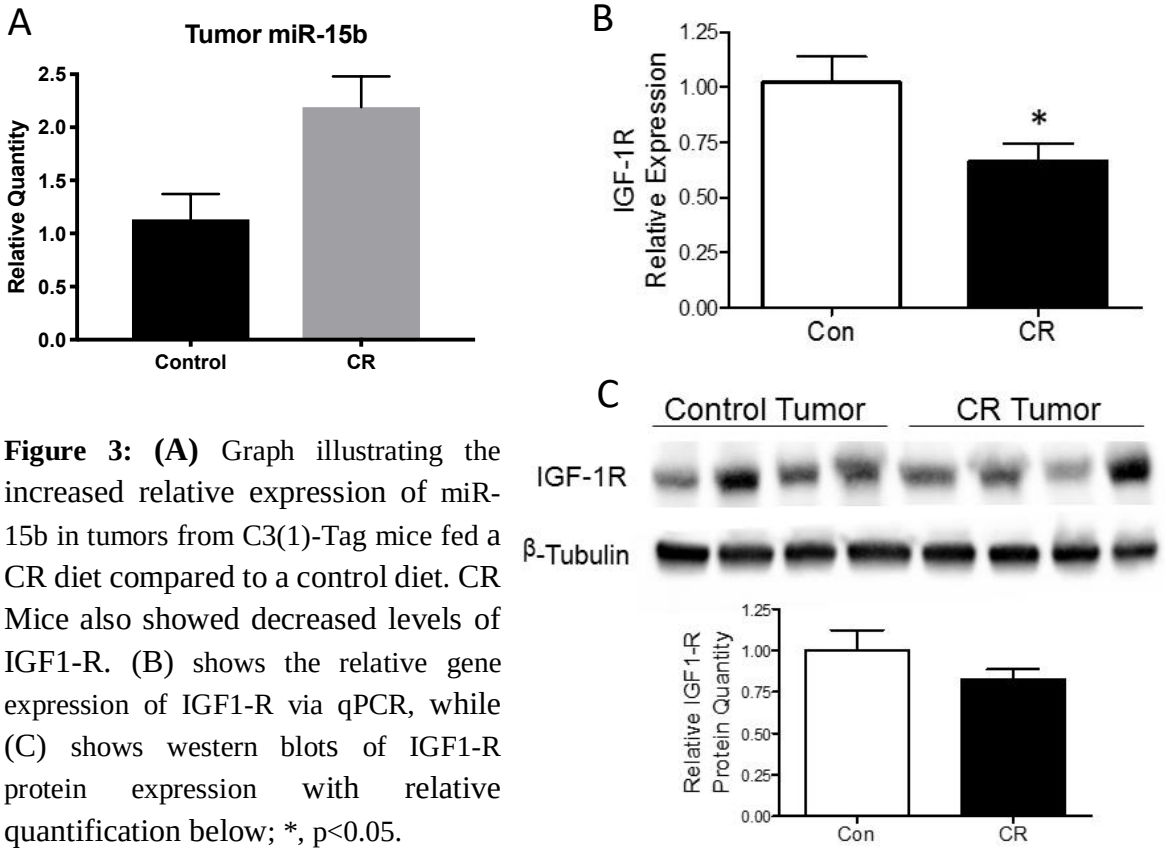

Figure 3: (A) Graph illustrating the increased relative expression of miR-15b in tumors from C3(1)-Tag mice fed a CR diet compared to a control diet. CR Mice also showed decreased levels of IGF1-R. (B) shows the relative gene expression of IGF1-R via qPCR, while (C) shows western blots of IGF1-R protein expression with relative quantification below; *, $p<0.05$.

Goals and Hypotheses

The goal of this project is to determine the role that miR-15b plays in the relationship between caloric restriction and triple-negative breast cancer in order to better understand the mechanisms underlying breast cancer development and metastasis. A more comprehensive understanding of these processes could potentially lead to newer and safer treatment plans for patients with TNBC to avoid the detrimental consequences of cytotoxic therapy.

Aim 1. Identify predicted targets of miR-15b and global effects of miR-15b expression in silico

miRNAs are responsible for a diverse, global range of regulatory effects within the cell, as each miRNA is suspected to target hundreds of mRNAs, even though miRNAs themselves compose only 0.01 % of all total RNA (24,25). Fortunately, there are bioinformatic databases with resources that can provide predicted gene targets of miRNAs, published literature on experimentally validated miRNA-target interactions, and molecular pathways they may be involved with. Analysis of this data will reveal how miR-15b and its predicted targets are involved in the PI3K/Akt/mTOR pathway signaling and oncogenic signaling regulation overall.

Aim 2. Determine the relationship between IGF-1 system activation and miR-15b

Two C3(1)-Tag progression series cell lines, the M6 and M6C cells, were cultured in various nutrient restricted cell medias and analyzed for alterations in both protein and gene expression. It is hypothesized that miR-15b expression will be upregulated in cells with greater nutrient restriction and that these changes will be more pronounced in the less aggressive cell lines. Furthermore, it is postulated that expression of genes and proteins involved in the activation of the PI3K/Akt/mTOR pathway will be reduced in cells with greater nutrient restriction and that regulation will correspond to the cell line's aggressiveness.

Methods

Gene Expression Analysis

For each sample, total RNA was first isolated from cells with the use of TRIzol reagent from ThermoFisher Scientific, which was utilized according to the manufacturer's instructions. The Omega Bio-Tek E.Z.N.A. Micro RNA Kit was used to extract pure fractions of both mRNA and miRNA simultaneously from the same samples with the use of spin columns according to the manufacturer's protocol. Both concentration and quality of miRNA and RNA collected from each sample were analyzed with the use of a Nanodrop 2000 spectrophotometer. For miRNA, cDNA was synthesized using the TaqMan Advanced miRNA cDNA Synthesis Kit according to manufacturer's instructions. For mRNA, cDNA was prepared using the Applied Biosystems High-Capacity cDNA Reverse Transcription Kit. qPCR reaction mixes were prepared using the TaqMan Universal Master Mix II paired with TaqMan Advanced miRNA assay (for miRNA) or TaqMan gene expression assay (for mRNA) in conjunction with RNase-free water and the synthesized cDNA. Assays were seeded in triplicate and run on an Applied Biosystems ViiA 7 Real-Time PCR system according to the instructions provided by the manufacturer. The ΔΔCt method was utilized to complete all relative expression calculations and generate an RQ value for each sample. The reference gene used for the miRNA analyses performed was miR-16-5p, while beta-actin as used for mRNA assays, as suggested by the manufacturer.

TargetScan/miRTarBase Analysis

The target prediction process first began with the generation of a consensus list of predicted targets using TargetScan Release 7.2 (26) .This program predicts gene target lists for specific miRNAs by attempting to find the best match between the conserved sequences of target genes and the seed region of a given miRNA (nucleotides 2-8). TargetScan then scores targets using the

context++ score measure of association, which ranks predictions based on their predicted targeting efficacy. Additionally, it scores targets with P_{CT} (probability of conserved targeting), a measure that further ranks targets based on their probability of targeting the seed sequence of a miRNA, a highly conserved region across most species. Based on previous literature and studies done using target prediction databases for miRNAs (27,28), a cutoff score of -0.3 for context++ score was set and only values below this score were accepted as potential targets. For P_{CT}, a cutoff score of 0.75 was used and only values above this were accepted as suitable targets. Using these parameters, the lists of predicted genes for the two mature forms of human and mouse miR-15b (hsa-miR-15b-5p, mmu-miR-15b-5p, hsa-miR-15b-3p, and mmu-miR-15b-3p) were filtered and compared. After this data was filtered, the narrowed list of potential gene targets was subject to further comparison in miRTarBase, a database that has stored more than 300,000 miRNA-gene target interactions that have been verified experimentally and published in the literature (29). In addition to miRTarBase analysis, the common gene targets of mmu-miR-15b-5p and hsa-miR-15b-5p obtained from TargetScan were also entered into the Database for Annotation, Visualization, and Integrated Discovery (DAVID) (29). DAVID performs a functional interpretation of entered gene lists to provide insight into which hallmark or oncogenic biochemical pathways the individual genes are a part of to determine the overall biological impact of changes in the gene list. It clusters separate genes into groups and shows the variety of pathways genes may be impacting along with the statistical significance of the probability that the pathway is being affected.

miR-15b Expression Correlation Analyses

Further target prediction analysis was completed with the use of MD Anderson Cancer Center's TCGA standardized data (32). TCGA is a public collection of molecular data sets generated using the tumors of over 10,000 cancer patients and accessible to cancer researchers

anywhere in the world for statistical analysis (31). This pool of data sets contains information about many tumor samples from various institutions at different times to discern genomic, proteomic, and transcriptomic trends that may be facilitating cancer-causing processes. In this instance, TCGA analysis via MD Anderson's collection of patient breast cancer tumor samples from their institutions was utilized in order to compare correlations in Reverse Phase Protein Array data (RPPA) and miR-15b expression along with correlations between miR-15b and Illumina RNA-sequencing (RNA-seq) data. By aligning the matrix data given for both RPPA and RNA-seq with miR-15b relative to breast cancer tumor samples, a protein list and gene list could both be generated and tested for significance of association with miR-15b. Lists were generated for both positive and negative correlating genes and proteins. Once significant gene and protein lists from the human tumor sample data were determined with the use of Pearson coefficient, T-value, p-value, and q-value statistics, the lists were each entered into DAVID to obtain functional interpretations of which pathways miR-15b may be playing a role in based on clustering and ranking of significant gene and protein groups. If results were insignificant, manual probing of the dataset was employed to examine lists and determine associations based on existing literature.

miR-15b Amplification Analyses

More *in silico* investigation of miR-15b's role in breast cancer was executed by probing human datasets on the human cancer data repository cBioPortal. It allows for download and visualization of these large-scale datasets for further analysis (32). Two of the largest breast cancer datasets, METABRIC (2509 samples) and TCGA BRCA (1084 samples) were probed for alterations in miR-15b. Then, gene expression was compared between tumor samples of patients with miR-15b alterations and those without. Genes that were significantly altered were then entered into Gene Set Enrichment Analysis (GSEA) online for pathway analysis. GSEA is a

computational method to show statistically significant relationships or differences between two biological states of a set gene list (33). In this analysis, overexpressed genes and under expressed genes were separated into different pools to maintain proper directionality of data. Specifically, both the Hallmarks gene sets and the C3 gene sets were observed in order to examine overall changes and C3 miRNA-specific changes, respectively. A flowchart summary of analyses using TCGA and METABRIC data can be seen in Figure 4.

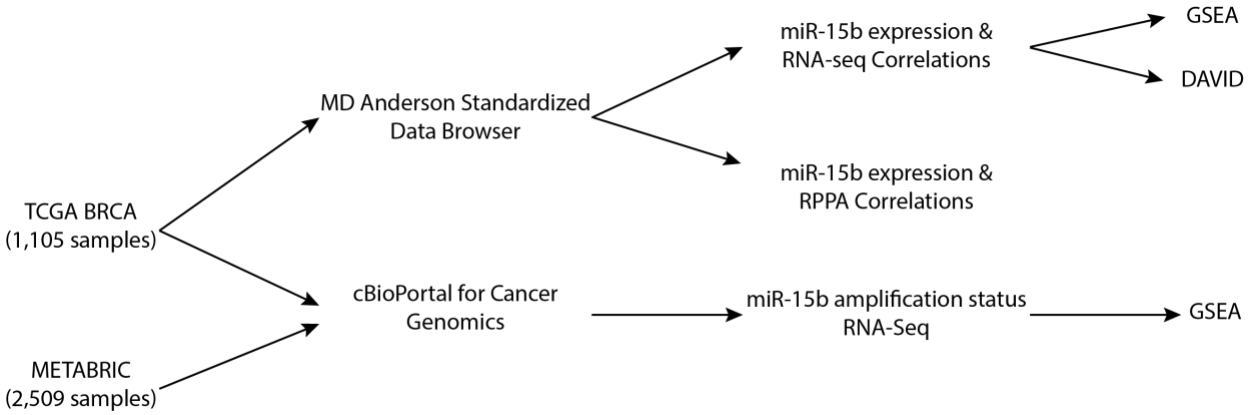

Figure 4: Flowchart depicting METABRIC and TCGA BRCA analyses.

Cell Culture

M6 and M6C cell lines were utilized for all *in vitro* experiments. These cell lines were generated following isolation of tumors from the C3(1)-Tag spontaneous model. The C3(1)-Tag transgenic line models basal-like breast cancer, and both the M6 and M6C cluster basal-like as well. The M6 and M6C are part of a larger progression series. The M6 was isolated from a primary C3(1)-Tag lesion, while the M6C was isolated from a lung metastatic nodule following subcutaneous injection of M6 cells into a nude mouse. M6 and M6C cell lines were cultured in high-glucose (25 mM) DMEM media supplemented with 10% FBS, 25 mM HEPES, 100 U/mL Pen/Strep, 1 mM Sodium Pyruvate, and 2 mM glutamine (complete media/CM). In order to mirror caloric restriction *in vitro*, ~300,000 cells of each C3-tag line were seeded into 6 cm plates containing and treated with one of the following treated media conditions for 18 hours: CM, CM

+ 100 nM BMS754807 (inhibitor of IGF1-R), Serum starvation (SS, CM with no FBS supplementation), SS + 10 ng/mL IGF-1, SS + BMS754807, and SS + 10 ng/mL IGF-1 + BMS754807. Cells were stored and maintained at 37°C in a 5% CO_2 humidified incubator.

Results

In Vitro Gene Expression Results

In order to characterize the role of caloric restriction on miRNA and mRNA involved in the PI3K/Akt/mTOR pathway in vitro, qPCR was utilized to profile relative expression of miR-15b and IGF1-R. It was hypothesized that miR-15b would have an inverse relationship with the aggressiveness of a cell line and IGF-1R would positively correlate with a cell line's aggressiveness based on previous pilot data. However, both qPCR of miR-15b and IGF1-R in various conditions of nutrient restriction revealed no significant differences in expression among cell lines. Results are displayed for miR-15b and IGF1-R expression in Figures 5A and 5B.

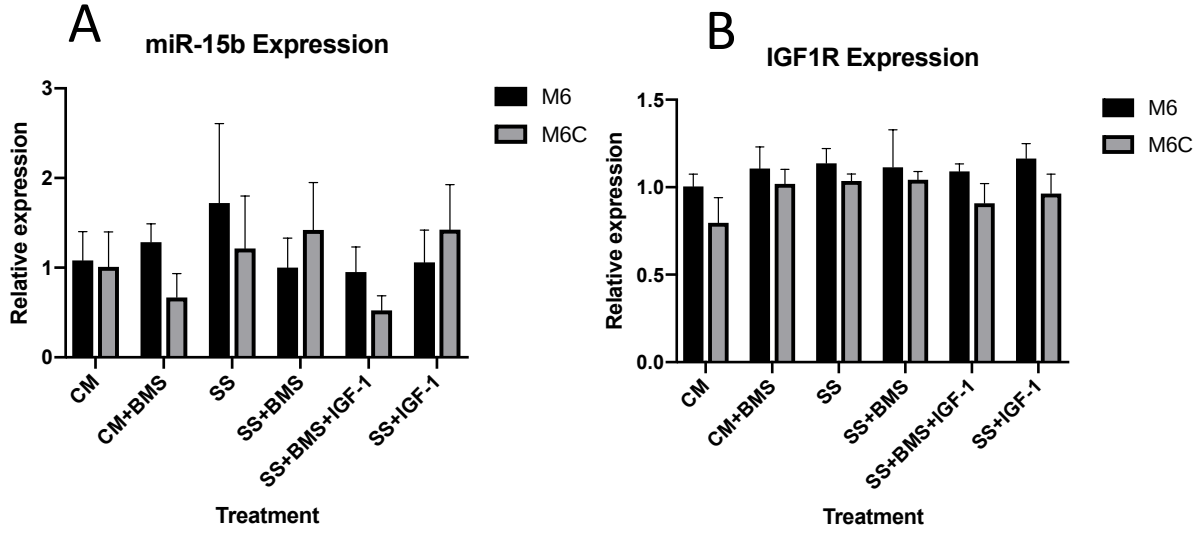

Figure 5A: Gene expression of miR-15b obtained via qPCR for both M6 (invasive carcinoma) and M6C (metastatic) cell lines.
Figure 5B: Gene expression of IGF1-R obtained via qPCR for both M6 (invasive carcinoma) and M6C (metastatic) cell lines.

***In Silico* Target Prediction Results**

Using TargetScan and the determined cutoff scores for context++ score and P_{CT}, a list of three genes was determined that overlap as potential targets of miR-15b in both mouse and human models. To gain a more comprehensive view of further genes that miR-15b potentially impacts, the gene list was filtered solely based on context++ score and this list expanded to six genes. This list included genes VAPB, TGIF2, UBE2Q1, ATXN7LS, TRANK1, and ATXN7LSB. Using miRTarBase, this expanded gene list was analyzed for any miR-15b gene-target interactions that have been verified experimentally. This analysis showed that both ATXN7LSB and TRANK1 had been confirmed *in vitro* via Next-Generation Sequencing (NGS*) in human samples. Additionally, ATXN7LSB has two publications discussing this gene-target interaction, while TRANK1 has three publications discussing this gene-target interaction. There were no mouse model gene-target interactions confirmed experimentally based on the list obtained from TargetScan analysis. Figure 6A displays the gene target alignment performed based on both context++ score and P_{CT}, while figure 6B shows the gene target alignment performed on the expanded gene list based only on context++score. Table 1 shows the results of the miRTarBase analysis that was performed.

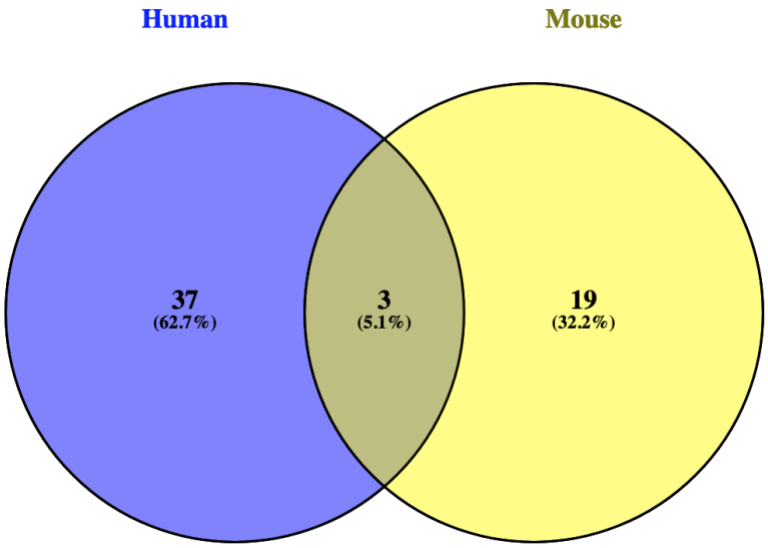

Figure 6A: Alignment for potential gene targets of miR-15b in both mouse and human models based on both context++ score and P_{CT}. The leftmost circle contains all the genes that met these criteria for humans, the rightmost circle contains all the genes that met these criteria for mice, and the middle overlap represents the number of genes in common between the two species.

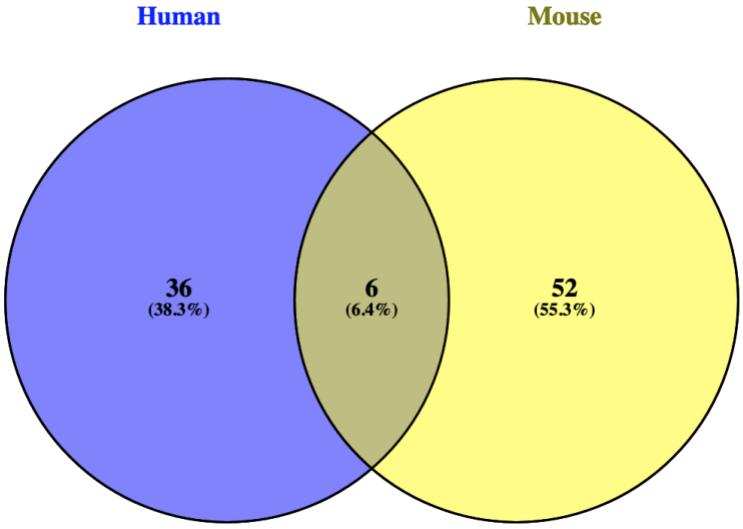

Figure 6B: Alignment for potential gene targets of miR-15b in both mouse and human models based on context++ score. The leftmost circle contains all the genes that met these criteria for humans, the rightmost circle contains all the genes that met these criteria for mice, and the middle overlap represents the number of genes in common between the two species.

Gene (human and mouse)	Reporter Assay	Western	qPCR	Microarray	NGS*	pSILAC	Other	Sum of methods	# of papers
ATXN7LSB								1	2
VAPB									
ATXN7LS									
TRANK1								1	3
UBEQ2									
TGIF2									

Table 1: miRTarBase was used to determine gene-target interactions confirmed in an array of different experiments. The NGS* results obtained were only confirmed in human samples. There were no confirmed interactions in the mouse model.

The results of cBioPortal analysis revealed several hallmark pathways miR-15b may be affecting, general and specific gene expression of samples with miR-15b amplification, and the overall relationship between IGF1-R and survival. Table 2 lists the top 15 significantly enriched pathways in genes significantly underexpressed in samples with miR-15b amplification compared to non-amplified samples. Pathways known to be involved in cancer growth and progression, such as estrogen signaling, fatty acid metabolism, and epithelial-to-mesenchymal transition, were all significantly decreased in samples with amplified miR-15b expression. In contrast, Table 3 shows the top 15 hallmark pathways in genes overexpressed in miR-15b amplified samples. Significantly associated pathways in these samples were also related to cancer proliferation, particularly that of cell cycle processes, and may indicate a more proliferative and less invasive phenotype in tumors with high levels of miR-15b. We also wanted to test how significantly affected genes in these samples fit with known targets of miRNA. Table 4 shows that, in samples with miR-15b amplification, we observe a significant decrease in gene expression of predicted target genes for miR-15b and its family of miRs. Additionally, we specifically wanted to see how miR-15b amplification affected IGF1R expression within breast tumors. Table 5 shows relative underexpression of IGF1-R in samples with miR-15b amplification compared to those without it. What is also striking about these data in tables 2-5 is the congruence between both the METABRIC and TCGA datasets, indicating that these are true differences observed in breast cancer and not an artifact of a single dataset. Lastly, cBioPortal analysis was able to provide Figure 7, which plotted the overall survival of breast cancer patients against expression of IGF1-R. The red line on the figure represents calculation of survival based on the gene query alteration for increased IGF1-R expression, and it illustrates a reduced probability of survival with increased IGF1-R expression.

Dataset	Gene Set Name	Genes in Overlap	FDR q-value
METABRIC	HALLMARK_ESTROGEN_RESPONSE_EARLY	75	3.80E-52
METABRIC	HALLMARK_ESTROGEN_RESPONSE_LATE	60	1.72E-35
TCGA BRCA	HALLMARK_ESTROGEN_RESPONSE_EARLY	42	2.42E-34
TCGA BRCA	HALLMARK_ESTROGEN_RESPONSE_LATE	25	6.52E-15
METABRIC	HALLMARK_FATTY_ACID_METABOLISM	28	1.22E-10
METABRIC	HALLMARK_HEME_METABOLISM	29	3.44E-09
METABRIC	HALLMARK_KRAS_SIGNALING_UP	29	3.44E-09
METABRIC	HALLMARK_P53_PATHWAY	29	3.44E-09
METABRIC	HALLMARK_EPITHELIAL_MESENCHYMAL_TRANSITION	28	1.13E-08
METABRIC	HALLMARK_BILE_ACID_METABOLISM	17	3.20E-06
TCGA BRCA	HALLMARK_P53_PATHWAY	13	1.31E-04
TCGA BRCA	HALLMARK_BILE_ACID_METABOLISM	8	2.87E-03
TCGA BRCA	HALLMARK_FATTY_ACID_METABOLISM	9	4.44E-03
TCGA BRCA	HALLMARK_HEME_METABOLISM	10	4.44E-03
TCGA BRCA	HALLMARK_KRAS_SIGNALING_UP	10	4.44E-03

Table 2: cBioPortal analysis of significantly underexpressed hallmark pathways in tumor samples with miR-15b amplification.

Dataset	Gene Set Name	Genes in Overlap	FDR q-value
METABRIC	HALLMARK_E2F_TARGETS	98	7.59E-88
TCGA BRCA	HALLMARK_E2F_TARGETS	65	2.33E-74
METABRIC	HALLMARK_G2M_CHECKPOINT	88	7.78E-74
TCGA BRCA	HALLMARK_G2M_CHECKPOINT	63	2.56E-71
METABRIC	HALLMARK_MTORC1_SIGNALING	58	1.13E-36
METABRIC	HALLMARK_MITOTIC_SPINDLE	54	1.66E-32
METABRIC	HALLMARK_MYC_TARGETS_V1	48	1.67E-26
TCGA BRCA	HALLMARK_MITOTIC_SPINDLE	32	6.90E-26
METABRIC	HALLMARK_INTERFERON_GAMMA_RESPONSE	44	9.37E-23
TCGA BRCA	HALLMARK_MTORC1_SIGNALING	27	5.77E-20
TCGA BRCA	HALLMARK_MYC_TARGETS_V1	26	6.58E-19
METABRIC	HALLMARK_UV_RESPONSE_UP	34	1.90E-17
METABRIC	HALLMARK_HYPOXIA	37	1.11E-16
METABRIC	HALLMARK_GLYCOLYSIS	30	2.28E-11
TCGA BRCA	HALLMARK_GLYCOLYSIS	18	1.38E-10

Table 3: cBioPortal analysis of significantly overexpressed hallmark pathways in tumor samples with miR-15b amplification.

Dataset	Gene Set Name	# Genes in Overlap (k)	FDR q-value
METABRIC	TGCTGCT_MIR15A_MIR16_MIR15B_MIR195_MIR424_MIR497	87	3.52E-25
TCGA BRCA	TGCTGCT_MIR15A_MIR16_MIR15B_MIR195_MIR424_MIR497	38	4.35E-12

Table 4: cBioPortal analysis of samples with miR-15b amplification, showing a significant decrease in gene expression of predicted target genes for miR-15b and its family of miRs

Dataset	Gene	Log Ratio	p-Value	q-Value	Tendency
METABRIC	IGF1R	-0.7	1.32E-05	3.99E-04	Under-expressed
TCGA BRCA	IGF1R	-1.21	2.33E-03	0.0325	Under-expressed

Table 5: cBioPortal analysis of relative underexpression of IGF1-R in samples with miR-15b amplification compared to those without it

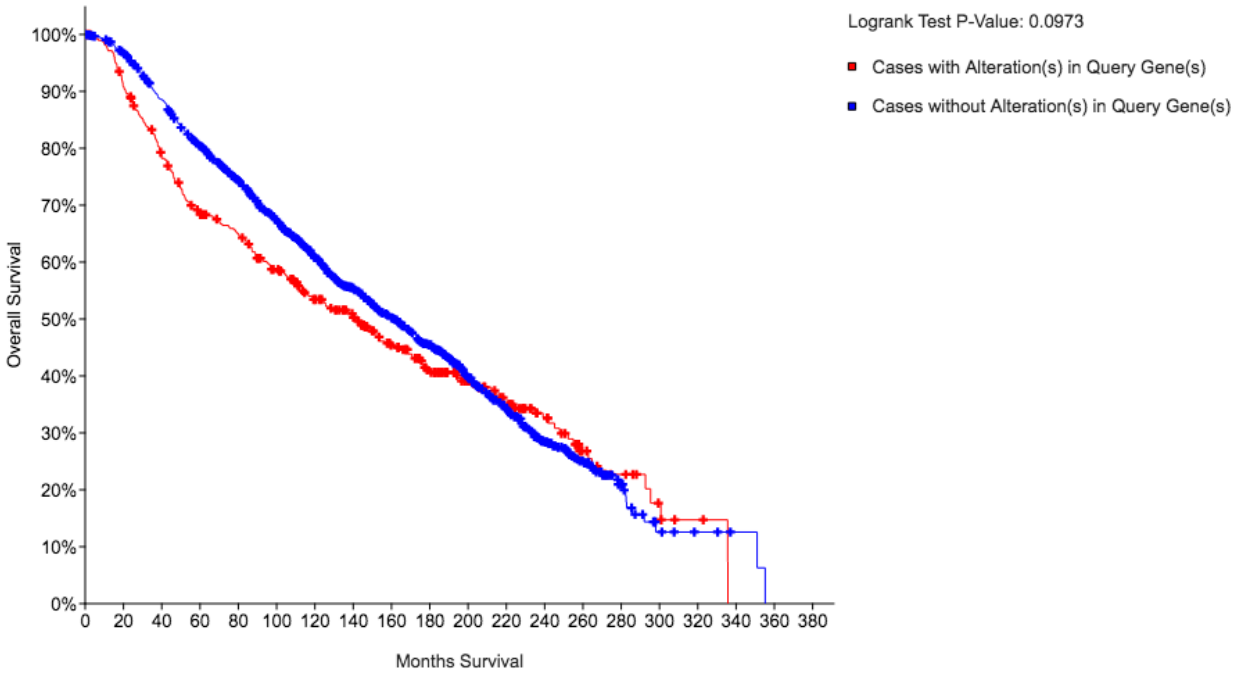

Figure 7: cBioPortal Analysis of the relationship between overall survival of breast cancer patients and relative IGF1-R expression. The red line indicates the decreased survival resulting from increased IGF1-R expression.

The results of DAVID analysis proved to be non-significant when performed on the list of genes predicted by TargetScan based on both P_{CT} and context++ score and on the list of genes predicted based only on context++ score. There was some correlation to important pathways that could be involved in cancer progression such as signaling peptides and transcription regulation, but none of these associations reached a p-value less than 0.1. DAVID analysis of the proteins significantly associated with miR-15b expression data from TCGA was insignificant for those

positively correlated and those negatively correlated, but manual clustering revealed positive association with cell cycle and proliferation and a negative association with growth factor signaling and breast cancer metastasis. These results are shown in Table 6. However, DAVID analysis of the significant gene lists positively and negatively correlating with miR-15b expression in samples had significant correlation with cancer development pathways. The results generally depict that miR-15b correlates with a down regulation of genes in growth-factor signaling processes and an upregulation of genes regulating cell proliferation. The pathways positively correlating with miR-15b expression are displayed in Table 7, and the pathways negatively correlating with miR-15b expression are shown in Table 8.

Protein	R Square	FDR q-value
EGFR_pY1173-R-V	-0.514259487	0.000031
Cyclin_B1-R-V	0.492487474	0.000031
YAP-R-E	-0.468007618	0.000102
PCNA-M-C	0.439580594	0.00025
eEF2-R-C	0.438557908	0.00025
Rictor_pT1135-R-V	-0.437895211	0.00025
c-Met_pY1235-R-V	-0.396591774	0.00076
IGF1R_pY1135_Y1136-R-V	-0.383495044	0.001078
STAT3_pY705-R-V	-0.352332655	0.002844
Caveolin-1-R-V	-0.324433726	0.006964
Cyclin_E1-M-V	0.296225823	0.013935
N-Cadherin-R-V	-0.24372596	0.043618
IRS1-R-V	-0.237074358	0.048504

Table 6: Manual clustering of the proteins significantly upregulated and downregulated with miR-15b expression in patient tumor samples.

Annotation Cluster 1	Enrichment Score: 65.58468325697848			
Category	Term	Count	%	PValue
UP_KEYWORDS	Cell cycle	114	37.74834437	3.16E-92
UP_KEYWORDS	Cell division	82	27.15231788	2.94E-71
UP_KEYWORDS	Mitosis	70	23.17880795	6.74E-68
GOTERM_BP_DIRECT	GO:0051301~cell division	74	24.50331126	3.89E-60
GOTERM_BP_DIRECT	GO:0007067~mitotic nuclear division	51	16.88741722	4.89E-40
Annotation Cluster 2	Enrichment Score: 30.647317611685196			
Category	Term	Count	%	PValue
UP_KEYWORDS	Centromere	41	13.57615894	3.37E-41
UP_KEYWORDS	Chromosome	55	18.21192053	1.57E-36
GOTERM_BP_DIRECT	GO:0007062~sister chromatid cohesion	34	11.25827815	8.12E-34
UP_KEYWORDS	Kinetochore	32	10.59602649	3.67E-33
GOTERM_CC_DIRECT	GO:0000777~condensed chromosome kinetochore	26	8.609271523	7.34E-25
GOTERM_CC_DIRECT	GO:0000776~kinetochore	21	6.953642384	1.13E-18
Annotation Cluster 3	Enrichment Score: 18.80465329639346			
Category	Term	Count	%	PValue
UP_KEYWORDS	DNA replication	28	9.271523179	7.43E-28
GOTERM_BP_DIRECT	GO:0000082~G1/S transition of mitotic cell cycle	26	8.609271523	1.32E-22
GOTERM_BP_DIRECT	GO:0006270~DNA replication initiation	15	4.966887417	2.97E-17
BIOCARTA	h_mcmPathway:CDK Regulation of DNA Replication	10	3.311258278	2.09E-10

Table 7: DAVID analysis of the pathways positively correlating with miR-15b expression in patient tumor samples.

Annotation Cluster 1	Enrichment Score: 12.305939606158537			
Category	Term	Count	%	PValue
UP_SEQ_FEATURE	signal peptide	72	41.61849711	2.54E-15
UP_KEYWORDS	Glycoprotein	82	47.39884393	4.41E-14
UP_SEQ_FEATURE	glycosylation site:N-linked (GlcNAc...)	79	45.66473988	1.20E-13
UP_KEYWORDS	Signal	76	43.93063584	4.30E-13
UP_SEQ_FEATURE	disulfide bond	59	34.10404624	5.00E-11
UP_KEYWORDS	Disulfide bond	64	36.99421965	5.06E-11
Annotation Cluster 2	Enrichment Score: 3.6650993586542997			
Category	Term	Count	%	PValue
UP_KEYWORDS	EGF-like domain	14	8.092485549	7.70E-08
INTERPRO	IPR000742:Epidermal growth factor-like domain	14	8.092485549	1.15E-07
INTERPRO	IPR013032:EGF-like, conserved site	13	7.514450867	1.71E-07
SMART	SM00181:EGF	13	7.514450867	1.47E-06
INTERPRO	IPR001881:EGF-like calcium-binding	10	5.780346821	1.65E-06
INTERPRO	IPR000152:EGF-type aspartate/asparagine hydroxylation site	9	5.202312139	3.68E-06
SMART	SM00179:EGF_CA	10	5.780346821	1.40E-05
INTERPRO	IPR018097:EGF-like calcium-binding, conserved site	8	4.624277457	3.00E-05
UP_SEQ_FEATURE	domain:EGF-like 8	5	2.89017341	6.00E-05
UP_SEQ_FEATURE	domain:EGF-like 1	8	4.624277457	6.60E-05
INTERPRO	IPR009030:Insulin-like growth factor binding protein, N-terminal	8	4.624277457	2.13E-04
Annotation Cluster 3	Enrichment Score: 2.6326343644289065			
Category	Term	Count	%	
UP_SEQ_FEATURE	topological domain:Extracellular	48	27.74566474	1.05E-06
UP_SEQ_FEATURE	topological domain:Cytoplasmic	51	29.47976879	3.44E-05
UP_KEYWORDS	Cell membrane	44	25.43352601	3.69E-04
GOTERM_CC_DIRECT	GO:0005886~plasma membrane	54	31.21387283	0.001232906
UP_SEQ_FEATURE	transmembrane region	59	34.10404624	0.003689304
GOTERM_CC_DIRECT	GO:0005887~integral component of plasma membrane	23	13.29479769	0.005777935
UP_KEYWORDS	Transmembrane helix	59	34.10404624	0.021812398

Table 8: DAVID analysis of the pathways negatively correlating with miR-15b expression in patient tumor samples.

Discussion

TargetScan/miRTarBase

Although the genes that miR-15b is predicted to target in both mouse and human models did not provide significant results when using TargetScan and miRTarBase, it has been recognized in previous literature that score prediction methods such as those of TargetScan should not be used so stringently when searching for potential gene-target interactions (34). When using cutoffs as a hard filter, there is potential for loss of real targets of miR-15b. This is because detection curves for matches to the conserved site initially increase at the same rate, but when conversed sites in the 5% most downregulated set are depleted, the detection rate for matches to the conserved site starts to level out. Therefore, a large number of downregulated targets (such as IGF1-R) can easily be missed when using these methods. These predictive scoring methods should be used in conjunction with other detailed measures.

Likewise, miRTarBase also should not be used as the only gauge of potential gene-target interactions. Although this database contains information from hundreds of thousands of miRNA functional studies, it is important to note that it only provides information on those that have been validated experimentally. Although it saves the researcher the burden of individually reviewing all relevant literature for a miRNA of interest, it is very possible that some of the predicted targets of miR-15b entered into miRTarBase simply have not been studied in enough detail yet. Therefore, it is unsurprising that miRTarBase was devoid of more information because it is likely that there are several more targets of miR-15b that simply lack experimental confirmation.

DAVID

The DAVID analyses performed only provided significant results for the genes obtained from the RNA-seq data that was correlated with miR-15b from the MD Anderson TCGA

Standardized Data Browser. It is likely that DAVID requires a large enough number of genes or proteins to be able to find significantly associated pathways because the RNA-seq data was comprised of 844 samples in comparison to the aligned RPPA proteins (92 samples) and the TargetScan gene list based on context++ score (41 samples).

However, manual clustering was still possible for the proteins significantly correlating both positively and negatively with miR-15b expression and these results were depicted in Table 6. This analysis revealed an upregulation of proteins involved with cell cycle and proliferation along with a downregulation of proteins involved in growth factor signaling and breast cancer metastasis. The results of the manual clustering were important not only because they provide confirmation of the data obtained through DAVID and GSEA analysis, but also because it showed a significant decrease in the number of phosphorylated growth factor receptors involved in major cell signaling pathways such as EGFR, HGFR, and most notably IGF1-R. This helps us verify how miR-15b may not only inhibit the receptor of these processes, but also system activation as a whole because it could be repressing downstream phosphorylation of key protein mediators of oncogenic mechanisms.

Table 7 illustrates the various pathways impacted by genes positively correlated with miR-15b expression. The clusters for positive correlation indicate that miR-15b may significantly increase genes involved in cell cycle regulation and various cell division processes. This is an important association because if miR-15b is increasing these regulatory genes, its protective effects could be the result of its influence on cell proliferation and development. With more genes for proper cell cycle completion, TNBC cells could have more difficulty evading its regulatory checkpoints, or could simply be in a more proliferative state compared to a more aggressive invasive state. Likewise, the impact of greater expression of genes involved in DNA replication

and mitosis could hinder the uncontrolled proliferation of TNBC cells. Table 8 shows the different pathways impacted by genes negatively correlated with miR-15b expression. These pathways seemed to be mostly related to epidermal growth-factor and other general signaling mechanisms. This table is critical to our hypothesis because if miR-15b is significantly altering IGF-1 system activation as predicted, then it is important that it is associated with a downregulation of genes involved with peptide or glycosylation signaling. These are two known methods by which pathways are able to transmit signals throughout the cell. Additionally, a negative association with epidermal growth factor (EGF) and its receptors was correlated with miR-15b overexpression. This is important to note because EGF has an analogous function to IGF-1 in terms of initiating tyrosine receptor phosphorylation cascades. In fact, EGF and IGF have been discovered to be closely associated in downstream signaling pathways related to therapy resistance in breast cancer, and there is likely significant crosstalk between EGF and IGF pathways (35).

cBioPortal

In Table 2, it was determined through cBioPortal analysis that the negatively correlating gene list was significantly associated with hallmark pathways in cancer development such as fatty acid metabolism, epithelial-to-mesenchymal transition (EMT), p53 pathway signaling, and KRAS pathway signaling. The downregulation of such pathways when exposed to miR-15b amplification are indicative of miR-15b's potentially antitumorigenic effects, and it highlights ways in which miR-15b may be accomplishing this outside the scope of just IGF-1 signaling pathways. Table 3 displays the list of upregulated hallmark pathways determined from the list of genes positively correlating with miR-15b. From this list, it is observed that pathways such as cell cycle regulation and cell division were upregulated based on the list of genes positively correlating with miR-15b.

This matches up with the pathways predicted to be upregulated after the alignment of RNA-seq data from MD Anderson's patient sample repository with miR-15b and analysis with DAVID. As mentioned before, this is important because miR-15b's potential influence on increasing genes implicated in cell cycle regulation could be important to discovering how it may be skipping regulatory checkpoints and proliferating without control.

Table 4 is a short but compelling figure because it is able to show that in samples with miR-15b amplification, we see significant downregulation of genes that are hypothesized to be targets of miR-15b and its related miRs. cBioPortal analysis was also able to provide table 5, which specifically looked at the impact of miR-15b's amplification on IGF1-R relative expression. In both datasets there was a significant decrease in IGF1-R expression, once again reinforcing the support for potential miR-15b mediated downregulation of IGF1-R. Furthermore, both the METABRIC dataset and the TCGA BRCA data sets depicted a very similar alterations in genes both over- and under-expressed in tumors with miR-15b amplification. This displays how there is concordance between both data sets and strong evidence for miR-15b's *in silico* predictions, as these findings are reproducible across two of the largest breast cancer datasets available.

Lastly, figure 7 provided a wholistic interpretation of IGF1-R's role in overall survival of TNBC patients. The graphic produced illustrated how greater relative expression of IGF1-R is may decrease overall survival in patients with breast cancer. This figure is important to consider because if miR-15b's antitumorigenic effects are taking place through inhibition of IGF1-R expression, it could also be playing an important role in the disease course of TNBC. By better understanding and confirming miR-15b's interactions with IGF1-R through experimentation, the full scope of its inhibitory capabilities could be realized and harnessed as a potential intervention for TNBC patients.

qPCR

Upon completion of qPCR for both the miRNA and mRNA obtained from all the samples exposed to differing nutrient conditions, it was determined that there were no significant differences between the control group and any of the nutrient restricted groups that were studied. Although the previous qPCR *in vivo* studies of C3-tag tumor samples conducted in our lab indicated a decrease in IGF1-R and an increase in miR-15b when exposed to caloric restriction (Figure 3A), the difference in such observed data could be due to something as basic as differences in the kit used for isolation. For example, there are other references in literature that suggest that depending on the protocol or brand name of kit used for isolation of miRNAs, reproducibility may vary between methods along with the quality and quantity of collected (36,37). Among various column-based kits such as the miRVana total RNA kit, the Norgen total RNA kit, and other standard non-kit extraction methods, there were differences in quantity of RNA collected up to 1000 ng/μL. The majority of 260/280 values were consistent for all methods outlined in this study, but 260/230 values had great variability and the total % of miRNA from all of these methods ranged from approximately 5-25%. In our past studies, total RNA was collected with the use of a RecoverAll™ total nucleic acid isolation kit. For this experiment, the Omega Bio-Tek E.Z.N.A. Micro RNA Kit was used which uses spin column-based methods to isolate miRNAs and larger RNAs into two separate fractions. Based on this outside literature, it is reasonable to conclude that differences in total RNA qPCR analysis for miRNAs vs separate qPCR analysis for miRNA and mRNA individually could yield alternate results. Furthermore, given the relatively lower abundance of miRNAs compared to mRNA and their uniquely small size, they are more difficult to amplify and more prone to the introduction of technical bias to results (38). Separating it from total RNA may have just been another means by which the sample could have been introduced to

more technical or random error. Utilizing a total RNA kit similar to the initial one used in pilot studies would have been more beneficial.

With greater time to work on my *in vitro* work, my second hypothesis could have been further examined with the use of western blotting protein analysis. Activation along the PI3K/Akt/mTOR pathway could have been experimentally validated by directly establishing levels of phospho-Akt, Akt, and IGF1-R proteins in each treatment group. It is necessary to use both methods to fully answer the question of IGF-1 system activation because as shown in other literature, transcriptional levels of mRNA and miRNA do not always correlate to the amount of protein translated (39,40). There are several post-transcriptional mechanisms taking place with other small RNAs other than miRNAs that can alter the amount of protein translation that occurs. Additionally, depending on which function they serve, certain subcategories of genes (such as those involved in cell signaling) tend to have differing levels of stable mRNA and stable protein. Therefore, mRNA and miRNA levels cannot be used as definite indicators of protein status without secondary confirmation.

Another *in vitro* component that could answer the question of whether or not miR-15b is truly driving IGF1-R repression is the use of small double-stranded mimetic RNA molecules. The use of mimetics can mimic levels of miRNA in the cell similar to the mature miRNA available from endogenous production (41). By elevating levels of miR-15b only, protein and RNA levels of IGF1-R could then be quantified in order to determine if its repression is specific to miR-15b or an alternate mechanism. If mimetics proved that IGF1-R's response to caloric restriction was in fact miR-15b specific, lentiviral transduction of a plasmid for stable miR-15b expression could be employed in the C3-Tag(1) progression cell lines to characterize how miR-15b's potential anti-tumorigenic effect is mediated in the cell and how it may differ across cells of increasing

tumorigenicity and metastatic capacity. Several methods such as colony-formation assays, flow cytometry for cancer stemness, migration assays, and invasion assays could then be performed on stable cell lines after lentiviral transduction to ascertain how miR-15b operates within the cell.

In conclusion, it was determined that miR-15b expression is positively associated with a proliferative gene signature and decreased growth factor phosphorylation, and it is negatively associated with growth factor signaling as well as classically pro-metastatic pathways. These findings were well supported due to their reproducibility across two large patient cohort data sets and in the context of both miR-15b expression and miR-15b amplification. Not only this, but data was also congruent between RNA-seq data and RPPA data obtained. Hopefully, future *in vitro* studies can help identify the exact mechanism of miR-15b's potential protective capabilities in TNBC. Elucidation of its mechanism could potentially lead to the design of newer and safer treatment plans in place of cytotoxic therapy and its detrimental health effects in patients diagnosed with TNBC.

Works Cited

1. Common Cancer Types [Internet]. National Cancer Institute. 2015 [cited 2019 Apr 1]. Available from: https://www.cancer.gov/types/common-cancers
2. How Common Is Breast Cancer? | Breast Cancer Statistics [Internet]. [cited 2019 Apr 1]. Available from: https://www.cancer.org/cancer/breast-cancer/about/how-common-is-breast-cancer.html
3. The First 5 Years: Recurrence Rate for Triple-Negative Breast Cancer [Internet]. Healthline. 2018 [cited 2019 Apr 1]. Available from: https://www.healthline.com/health/triple-negative-breast-cancer-recurrence
4. Street W. Breast Cancer Facts & Figures 2017-2018. :44.
5. Zeichner SB, Terawaki H, Gogineni K. A Review of Systemic Treatment in Metastatic Triple-Negative Breast Cancer. Breast Cancer Basic Clin Res. 2016 Mar 22;10:25–36.
6. Picon-Ruiz M, Morata-Tarifa C, Valle-Goffin JJ, Friedman ER, Slingerland JM. Obesity and adverse breast cancer risk and outcome: Mechanistic insights and strategies for intervention. Ca. 2017;67(5):378–97.
7. Trivers KF, Lund MJ, Porter PL, Liff JM, Flagg EW, Coates RJ, et al. The epidemiology of triple-negative breast cancer, including race. Cancer Causes Control CCC. 2009 Sep;20(7):1071–82.
8. Chan DSM, Norat T. Obesity and breast cancer: not only a risk factor of the disease. Curr Treat Options Oncol. 2015 May;16(5):22.
9. Simone B, Ko K, Nowak K, Rese A, Venkataraman C, Andrews DW, et al. Obesity Drives Prognosis in Women with Metastatic Breast Cancer. Int J Radiat Oncol. 2017 Oct;99(2):E46.
10. Bousquenaud M, Fico F, Solinas G, Rüegg C, Santamaria-Martínez A. Obesity promotes the expansion of metastasis-initiating cells in breast cancer. Breast Cancer Res BCR [Internet]. 2018 [cited 2019 Apr 1];20. Available from: https://www.ncbi.nlm.nih.gov/pmc/articles/PMC6123990/
11. O'Flanagan CH, Smith LA, McDonell SB, Hursting SD. When less may be more: calorie restriction and response to cancer therapy. BMC Med [Internet]. 2017 May 24 [cited 2019 Apr 1];15. Available from: https://www.ncbi.nlm.nih.gov/pmc/articles/PMC5442682/
12. Simone BA, Dan T, Palagani A, Jin L, Han SY, Wright C, et al. Caloric restriction coupled with radiation decreases metastatic burden in triple negative breast cancer. Cell Cycle. 2016 Mar 30;15(17):2265–74.
13. Nutrition, insulin, IGF-1 metabolism and cancer risk: a summary of epidemiological evidence. - PubMed - NCBI [Internet]. [cited 2019 Apr 1]. Available from: https://www.ncbi.nlm.nih.gov/pubmed/15562834
14. Chitnis MM, Yuen JSP, Protheroe AS, Pollak M, Macaulay VM. The type 1 insulin-like growth factor receptor pathway. Clin Cancer Res Off J Am Assoc Cancer Res. 2008 Oct 15;14(20):6364–70.
15. Kaaks R. Nutrition, insulin, IGF-1 metabolism and cancer risk: a summary of epidemiological evidence. Novartis Found Symp. 2004;262:247–60; discussion 260-268.
16. Wu Y, Cui K, Miyoshi K, Hennighausen L, Green JE, Setser J, et al. Reduced circulating insulin-like growth factor I levels delay the onset of chemically and genetically induced mammary tumors. Cancer Res. 2003 Aug 1;63(15):4384–8.

17. Sell C, Rubini M, Rubin R, Liu JP, Efstratiadis A, Baserga R. Simian virus 40 large tumor antigen is unable to transform mouse embryonic fibroblasts lacking type 1 insulin-like growth factor receptor. Proc Natl Acad Sci U S A. 1993 Dec 1;90(23):11217–21.
18. Davison Z, de Blacquière GE, Westley BR, May FEB. Insulin-like growth factor-dependent proliferation and survival of triple-negative breast cancer cells: implications for therapy. Neoplasia N Y N. 2011 Jun;13(6):504–15.
19. Christopoulos PF, Msaouel P, Koutsilieris M. The role of the insulin-like growth factor-1 system in breast cancer. Mol Cancer [Internet]. 2015 Feb 15 [cited 2019 Apr 1];14. Available from: https://www.ncbi.nlm.nih.gov/pmc/articles/PMC4335664/
20. MacFarlane L-A, Murphy PR. MicroRNA: Biogenesis, Function and Role in Cancer. Curr Genomics. 2010 Nov;11(7):537–61.
21. Fang Z, Rajewsky N. The impact of miRNA target sites in coding sequences and in 3'UTRs. PloS One. 2011 Mar 22;6(3):e18067.
22. Catalanotto C, Cogoni C, Zardo G. MicroRNA in Control of Gene Expression: An Overview of Nuclear Functions. Int J Mol Sci [Internet]. 2016 Oct 13 [cited 2019 Apr 1];17(10). Available from: https://www.ncbi.nlm.nih.gov/pmc/articles/PMC5085744/
23. Pratt AJ, MacRae IJ. The RNA-induced Silencing Complex: A Versatile Gene-silencing Machine. J Biol Chem. 2009 Jul 3;284(27):17897–901.
24. Lim LP, Lau NC, Garrett-Engele P, Grimson A, Schelter JM, Castle J, et al. Microarray analysis shows that some microRNAs downregulate large numbers of target mRNAs. Nature. 2005 Feb 17;433(7027):769–73.
25. Huntzinger E, Izaurralde E. Gene silencing by microRNAs: contributions of translational repression and mRNA decay. Nat Rev Genet. 2011 Feb;12(2):99–110.
26. TargetScanHuman 7.2 [Internet]. [cited 2019 Apr 1]. Available from: http://www.targetscan.org/vert_72/
27. Riffo-Campos ÁL, Riquelme I, Brebi-Mieville P. Tools for Sequence-Based miRNA Target Prediction: What to Choose? Int J Mol Sci [Internet]. 2016 Dec 9 [cited 2019 Apr 1];17(12). Available from: https://www.ncbi.nlm.nih.gov/pmc/articles/PMC5187787/
28. Agarwal V, Bell GW, Nam J-W, Bartel DP. Predicting effective microRNA target sites in mammalian mRNAs. eLife [Internet]. [cited 2019 Apr 1];4. Available from: https://www.ncbi.nlm.nih.gov/pmc/articles/PMC4532895/
29. miRTarBase: the experimentally validated microRNA-target interactions database [Internet]. [cited 2019 Apr 1]. Available from: http://mirtarbase.mbc.nctu.edu.tw/php/index.php
30. DAVID Functional Annotation Bioinformatics Microarray Analysis [Internet]. [cited 2019 Apr 1]. Available from: https://david.ncifcrf.gov/
31. Deng M, Brägelmann J, Schultze JL, Perner S. Web-TCGA: an online platform for integrated analysis of molecular cancer data sets. BMC Bioinformatics [Internet]. 2016 Feb 6 [cited 2019 Apr 13];17. Available from: https://www.ncbi.nlm.nih.gov/pmc/articles/PMC4744375/
32. cBioPortal for Cancer Genomics [Internet]. [cited 2019 Apr 2]. Available from: https://www.cbioportal.org/
33. GSEA [Internet]. [cited 2019 Apr 2]. Available from: http://software.broadinstitute.org/gsea/index.jsp
34. Betel D, Koppal A, Agius P, Sander C, Leslie C. Comprehensive modeling of microRNA targets predicts functional non-conserved and non-canonical sites. Genome Biol. 2010;11(8):R90.

35. Castaño Z, Marsh T, Tadipatri R, Kuznetsov HS, Al-Shahrour F, Paktinat M, et al. Stromal EGF and igf-I together modulate plasticity of disseminated triple-negative breast tumors. Cancer Discov. 2013 Aug;3(8):922–35.
36. El-Khoury V, Pierson S, Kaoma T, Bernardin F, Berchem G. Assessing cellular and circulating miRNA recovery: the impact of the RNA isolation method and the quantity of input material. Sci Rep. 2016 Jan 20;6:19529.
37. Brown RAM, Epis MR, Horsham JL, Kabir TD, Richardson KL, Leedman PJ. Total RNA extraction from tissues for microRNA and target gene expression analysis: not all kits are created equal. BMC Biotechnol [Internet]. 2018 Mar 16 [cited 2019 Apr 1];18. Available from: https://www.ncbi.nlm.nih.gov/pmc/articles/PMC5857145/
38. Practical data handling pipeline improves performance of qPCR-based circulating miRNA measurements [Internet]. [cited 2019 Apr 1]. Available from: https://www.ncbi.nlm.nih.gov/pmc/articles/PMC5393188/
39. Kendrick N, Laboratories K, St A. A gene's mRNA level does not usually predict its protein level. :8.
40. Maier T, Güell M, Serrano L. Correlation of mRNA and protein in complex biological samples. FEBS Lett. 2009 Dec 17;583(24):3966–73.
41. Wahid F, Shehzad A, Khan T, Kim YY. MicroRNAs: Synthesis, mechanism, function, and recent clinical trials. Biochim Biophys Acta BBA - Mol Cell Res. 2010 Nov 1;1803(11):1231–43.